

# ACCELERATING DATA ACQUISITION FOR REVERSED-GRADIENT DISTORTION CORRECTION IN DIFFUSION MRI: A CONSTRAINED RECONSTRUCTION APPROACH

Chitresh Bhushan<sup>1</sup>, Anand A Joshi<sup>1</sup>, Richard M Leahy<sup>1</sup>, and Justin P Haldar<sup>1</sup>

<sup>1</sup>Signal and Image Processing Institute, University of Southern California, Los Angeles, CA, United States

**Introduction** – The EPI readouts used to acquire most diffusion weighted images (DWIs) are well known to produce localized geometric distortions in the presence of  $B_0$  field inhomogeneity. These artifacts, which manifest as local stretching or compression of the image along the phase encoding (PE) direction, are problematic when attempting to co-register diffusion images with other scans or attempting to estimate diffusion characteristics in highly-distorted regions. Geometric distortions can be accurately predicted from the  $B_0$  inhomogeneity map, and many methods use measured field maps to partially correct distortions [1]. However, these corrections are of limited use in image regions where the distortions have superposed signals from multiple different spatial locations. The reversed-gradient (RG) method [2], in which images are acquired with two different PE orientations (PEOs), can overcome these effects at the expense of doubling the data acquisition time. This work proposes a novel acquisition and reconstruction strategy that leverages a constrained reconstruction formulation to enable accurate RG distortion correction from only half the amount of data required for the standard RG approach.

**Theory** – Reversing the orientation of the PE gradient in EPI causes stretching artifacts to become compression artifacts, and vice versa. As illustrated in Fig. 1, acquiring two PEOs enables better artifact correction than can be obtained from a single PEO. Compared to conventional RG, which acquires every image with two PEOs, we propose to reduce the scan time by acquiring half the images with one PEO and half with the other. Distortion correction of these images is then performed jointly, using a constrained reconstruction formulation that uses the prior knowledge that the diffusion signal in each voxel should be smooth in  $q$ -space.

**Materials and Methods** – We assume a DWI acquisition with spherical  $q$ -space sampling, and choose PEOs for each DWI in an interleaved fashion (as shown in Fig. 2, where white dots and black dots correspond to different PEOs). We use the acquired distorted diffusion images ( $\mathbf{d}_q$ ) to estimate undistorted images ( $\mathbf{s}_q$ ) by minimizing

$\sum_q \|\mathbf{D}_q \mathbf{s}_q - \mathbf{d}_q\|^2 + \alpha_1 \sum_v \|\mathbf{L} \mathbf{c}_v\|^2 + \alpha_2 R(\mathbf{s}_1, \dots, \mathbf{s}_q)$  s.t.  $\mathbf{s}_{qv} = \mathbf{Y}_q \mathbf{c}_v$ , where, subscripts  $q$  and  $v$  correspond to different diffusion encodings and voxels, respectively.  $\mathbf{D}_q$  is the matrix that performs deformation (or distortion) according to a measured field map and knowledge of the PEO;  $\mathbf{L}$  is the Laplace-Beltrami operator in the spherical harmonic (SH) domain, which we use to impose smoothness on the sphere in  $q$ -space [3];  $\mathbf{c}_v$  is the vector of SH coefficients for the  $v$ th voxel;  $\mathbf{Y}$  is a matrix that converts SH coefficients into samples on the sphere in  $q$ -space;  $R(\cdot)$  is a spatial regularization term (e.g., [4]); and  $\alpha_1$  and  $\alpha_2$  are empirically tuned regularization parameters. We minimize this cost function using the iterative LSQR algorithm.

To evaluate the proposed method, we acquired a standard RG 20-direction diffusion dataset for a single subject (single-shot EPI, TE=88ms, TR=10s, b=1000s/mm<sup>2</sup>, 2x2x2mm<sup>3</sup>), along with a  $B_0$  inhomogeneity map. From this data, we subsampled the RG dataset in an interleaved fashion so that each DWI was only sampled with one PEO and the PEOs were distributed uniformly in  $q$ -space.

**Results** – Figs. 3 and 4 compare the performance of distortion correction using (i) the proposed method, (ii) the proposed method with  $\alpha_1 = 0$ , and (iii,iv) the standard single-PEO method [1] with each of the two different PEOs. Performance is measured with respect to the standard RG method [2] that uses twice the data. Fig. 3 shows the maximum intensity projection (MIP) of the absolute image reconstruction errors, while Fig. 4 shows MIPs of the fractional anisotropy (FA) errors computed from a diffusion tensor fit. The single PEO methods perform poorly in the frontal and temporal lobes, which are severely affected by the distortion. We see a marginal improvement in performance when the proposed method is used without the  $q$ -space smoothness constraint. We get a significant improvement when  $q$ -space smoothness constraints are included.

**Conclusion** – We have proposed an accelerated distortion correction method for diffusion MRI, which benefits from RG acquisition but without increasing the scan time. We have demonstrated that the performance of the proposed method is similar to that of the standard RG method both in terms of the reconstructed images and quantitative diffusion measures. The proposed method requires a simple modification of a standard diffusion acquisition, in which half the data is acquired with a PEO that is opposite to the PEO of the other half.

**References** – [1] Jezzard, *Magn Reson Med* 1995; 34:65-73. [2] Andersson, *NeuroImage* 2003; 20:870-888. [3] Descoteaux, *Magn Reson Med* 2007;58:497-510. [4] Haldar, *Magn Reson Med* 2012; In Press, doi:10.1002/mrm.24229.

**Grant Support** – This work was supported in part by: NIH-P41-RR013642, NIH-EB000473, NIH-R01-NS074980, NIH-P50-NS019632.

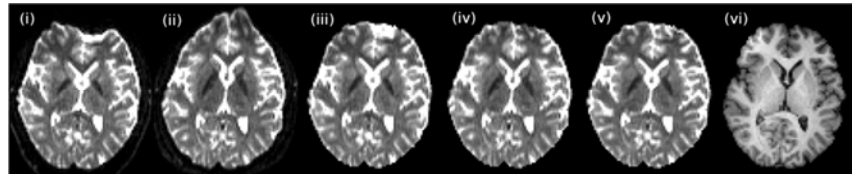


Figure 1: Images distorted with different PEOs (i) & (ii) were each corrected using a field map [1] to get (iii) & (iv) respectively; (v) corrected using RG method; (vi) anatomical reference (MPRAGE).

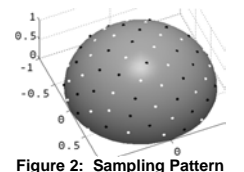


Figure 2: Sampling Pattern

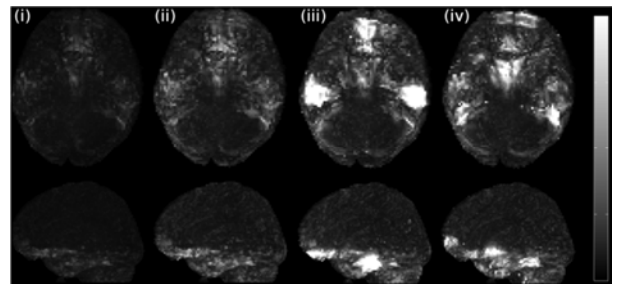


Figure 3: MIP images of DWI errors (a.u.). Top: axial MIP. Bottom: sagittal MIP.

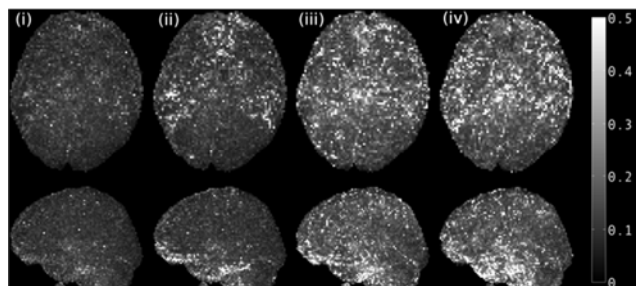


Figure 4: MIP images of FA errors. Top: axial MIP. Bottom: sagittal MIP.